

The Macronova in GRB 050709 and the GRB/macronova connection

Zhi-Ping Jin,¹ Kenta Hotokezaka,² Xiang Li,^{1,3} Masaomi Tanaka,⁴ Paolo D'Avanzo,⁵ Yi-Zhong Fan*,^{1,6} Stefano Covino*,⁵ Da-Ming Wei,¹ and Tsvi Piran*²

¹*Key Laboratory of Dark Matter and Space Astronomy,
Purple Mountain Observatory, Chinese Academy of Sciences, Nanjing 210008, China*

²*Racah Institute of Physics, The Hebrew University, Jerusalem, 91904, Israel*

³*University of Chinese Academy of Sciences, Yuquan Road 19, Beijing, 100049, China*

⁴*National Astronomical Observatory of Japan, Mitaka, Tokyo 181-8588, Japan*

⁵*INAF/Brera Astronomical Observatory, via Bianchi 46, I-23807 Merate (LC), Italy*

⁶*Collaborative Innovation Center of Modern Astronomy and Space Exploration,
Nanjing University, Nanjing, 210046, China*

GRB 050709 was the first short Gamma-ray Burst (sGRB) with an identified optical afterglow. In this work we report a re-analysis of the publicly available data of this event and the discovery of a Li-Paczynski macronova/kilonova that dominates the optical/IR signal at $t > 2.5$ days. Such a signal would arise from $0.05 M_{\odot}$ r-process material launched by a compact binary merger. The implied mass ejection supports the suggestion that compact binary mergers are significant and possibly main sites of heavy r-process nucleosynthesis. We have re-analyzed all afterglow data from nearby short and hybrid GRBs. A statistical study of sGRB/macronova connection reveals that macronova may have taken place in all these GRBs though the fraction as low as 0.18 cannot be ruled out. The identification of two of the three macronova candidates in the I-band implies a more promising detection prospect for ground-based surveys.

PACS numbers: 98.70.Rz, 04.25.dg, 97.60.Jd

I. INTRODUCTION

Compact object mergers are strong sources of gravitational waves (GW) and are prime targets for the advanced LIGO/Virgo detectors [1, 2]. It has been suggested that short Gamma-ray Bursts (sGRBs) arise from mergers in which one of the compact objects is a neutron star [3], a scenario now favored by a broad range of observations (see e.g. [4, 5]). In the absence of GW detection, a clear signature for the compact-binary origin of a sGRB is a Li-Paczynski macronova/kilonova: a near-infrared (nIR)/optical transient powered by the radioactive decay of r -process material synthesized in ejecta launched during the merger [6–18].

To date, the evidence of a macronova associated with sGRB 130603B is based on only a single data point [19, 20]. The peculiar GRB 060614 was denoted as a “hybrid burst”, since its $T_{90} \approx 102$ s groups it with long-duration GRBs, while its temporal lag and peak luminosity are within the short-duration GRB subclass [21]. Moreover there is no evidence for an associated supernova emission [22–24] down to very stringent limits. The most significant macronova evidence within this afterglow is due to a single Hubble Space Telescope (HST) observation at $t \sim 13.6$ days after the burst [25]. Further explorations of the afterglow allowed us to derive a tentative macronova light curve [26]. In search for further evidence for other macronovae we explored the optical/IR afterglows of all other nearby short and hybrid GRBs (hGRBs) in which macronova signals could have been detected. We begin with the study of GRB 050709, the first sGRB with an identified optical afterglow. Previous works have found irregularity in this afterglow and inter-

preted it as a jet break [27] or as an optical flare [28]. Re-analyzing the previous observations we suggest here that this irregularity arises due to a macronova component which in fact dominates the afterglow light curve in this burst. We then compare it with other GRBs/macronovae and explore the implications of these results to the short-GRB/macronova connection.

We have identified a possible macronova in the optical afterglow data of sGRB 050709. The I -band light curve of this macronova candidate is remarkably similar to that of the macronova candidate of hGRB 060614 [25, 26], even though the isotropic-equivalent energy ($E_{\gamma, \text{iso}}$) of their prompt emission and the X-ray afterglow light curve are significantly different. Examination of the late-time optical–nIR data of all nearby short and hGRBs ($z < 0.4$) for which a macronova could have been observed (six in total) revealed that there are three events GRBs 050709, 060614, and 130603B in which a macronova candidate has been detected. The three other events don’t show such a signal but for each one of them there are concerns that explain this away. The appearance of a macronova candidate in three out of three (or at most six) events suggest that macronovae are ubiquitous. This supports strongly the hypothesis that compact binary mergers that are accompanied by sGRBs, are the prime sites of heavy r-process nucleosynthesis. The identifications of two of those macronova candidates in the I -band suggest that macronova could be more easily detected in GW follow-up searches, even without a GRB trigger.

II. RESULTS

A. A macronova signal associated with GRB 050709

GRB 050709 was detected by the NASA’s High Energy Transient Explorer (HETE-2) and was localized by the HETE-2’s Soft X-ray Camera [29]. Its prompt emission consisted of a hard spike (~ 0.5 s) and an extended X-ray emission lasting ~ 130 s [29]. The accurate localization led to follow-up observations allowed to identify the first optical afterglow of a short gamma-ray burst [27, 30, 31]. About 1.5 days after the trigger of sGRB 050709, Hjorth et al. [30] observed it with the *Danish* 1.54m telescope. They reported two *R*-band detections. Fox et al. [27] obtained four HST exposures in the F814W-band. The HST observed the site of sGRB 050709 one year later in the same band and didn’t detect any signal. Covino et al. [31] observed the source with the Very Large Telescope (VLT) in *V/R/I* bands and detected the afterglow in *V* and *R* bands simultaneously on Jul. 12.4 UT. The optical afterglow that was localized with sub-arcsecond accuracy was in the outskirts of an irregular, late-type galaxy at a redshift of 0.16 [27, 30]. The host’s star-formation rate, $\sim 0.2 M_{\odot} \text{ yr}^{-1}$, is much higher than that of the hosts of the two other sGRBs detected at the time, i.e. 050509B and 050724, and it renders GRB 050709 to be the first sGRB occurring in a star forming “low-luminosity” galaxy [30, 31]. The X-ray afterglow observations of sGRB 050709 are scarce. At $t > 200$ s there are only two significant detections by Chandra (including an X-ray flare at $t \sim 16$ days). Two other *Swift* ($t \sim 1.6$ days) and Chandra ($t \sim 16.1$ days) data points have a significance of $\sim 2\sigma$ [27]. No radio afterglow emission has been detected [27].

Already in 2005, Fox et al. [27] noted that the early HST optical/IR data declined as $t^{-1.25 \pm 0.09}$ and then it dropped as $t^{-2.83 \pm 0.39}$ between 10 and 20 days. They suggested that this arose due to a jet break. This interpretation was valid for the HST data set available at that time. Later, Watson et al. [28] combined the optical/near-infrared (nIR) data from the Danish 1.54m telescope, VLT and HST, and showed that the decline is much faster: a single power law of $t^{-1.73 \pm 0.04}$. A single HST data point at $t \sim 9.8$ days was significantly above this line and this was interpreted as a flare powered by a central engine activity. Following a re-analysis of all publicly available data we show that the light curve is chromatic and this rules out an afterglow scenario (e.g. a jet break). We find a strong evidence for the presence of a new emission component besides the regular forward shock emission and that this component is strong not just at $t \sim 9.8$ days but also at earlier times. We compare the light curve to the predictions of macronova estimates and we suggest that this nIR excess lasting ~ 10 days indicates a macronova emission.

We have analyzed all publicly-available optical/nIR data of the afterglow of sGRB 050709 (see the Methods for the details). Results of our re-analysis are generally

consistent with those reported in the literature [27, 31]. For the VLT data at ~ 2.5 days, we confirm the detection in *R* and *V* bands. However, while previous analysis of this data yielded only an upper limit of 23.25 mag [31] our reanalysis of the VLT *I*-band at $t \sim 2.5$ days resulted in a detection with a Vega magnitude of 24.1 ± 0.2 (see the Methods for a detailed discussion of this analysis). This *I*-band observation was almost coincidental with the *R* and *V* observations with which we can reliably estimate the energy distribution of the spectrum (SED). We have also found an unpublished Gemini optical observation giving a tight 3σ upper limit of 25.4 mag on the *R*-band flux at $t \sim 6.6$ days after the burst.

The Fig.1(a) depicts all the available optical/nIR data. The *R*-band emission decreases as $t^{-1.63 \pm 0.16}$. This is consistent with the *V*-band data and with the overall fit of Watson et al. [28]. Note that the new *R* band upper limit (at $t \sim 6.6$ days) is consistent with the Watson et al. [28]’s fit. On the other hand the *I*-band emission decreases much slower, as of $t^{-1.12 \pm 0.09}$, and this is consistent with the Fox et al. [27]’s analysis of the early HST data alone. The standard afterglow model, implies an achromatic decay and hence the different behavior in the *R* and *I* bands over a long timescale of ~ 10 days is inconsistent with an afterglow model [33]. In fact attempt to fit all the *I* and *R* band observations to a single achromatic broken power fails, with the best χ -square p.d.f. obtained is of order 10 (ignoring the HST data point at $t \sim 18.7$ days does not solve the problem). This strongly suggests an additional component.

Further information is obtained from the puzzling spectrum at $t \sim 2.5$ days. Here, the *R* band flux is significantly larger than the *I* band flux. This again is inconsistent with a standard afterglow model and it suggests that an additional component dominates already at this stage. Namely, any afterglow emission is subdominant already at $t \sim 2.5$ days. This can happen if there was an early jet break at $t \lesssim 1.4$ days, in which case the afterglow would have declines from its observed value at $t = 1.4$ days as t^{-p} , with $p > 2$. Such a decline (with $p = 2.5$, which is consistent with the X-ray spectrum) is also shown in Fig.1. Indeed, for $p = 2.5$ and the cooling frequency $\nu_c \sim 2.5 \times 10^{16}$ Hz at $t \sim 2.5$ days, the extrapolation of the Chandra X-ray emission into optical bands yields emission flux lower than the VLT data, consistent with the presence of a macronova emission component. Both the required fast decline rate as well as the jet break time are consistent with that observed in some other sGRBs and in particular in sGRB 130603B and hGRB 060614 [19, 20, 34], two events displaying macronova signals. Remarkably, even without the VLT *I*-band data, Watson et al. [28] already noticed that the decline is rather steep suggesting a post jet break afterglow and that at $t \sim 10$ days the HST F814W-band emission was in excess of the regular forward shock afterglow emission. With the new data points the evidence for a macronova signal is much stronger. Remarkably, this *I*/F814W macronova signal (see Fig.2, where the

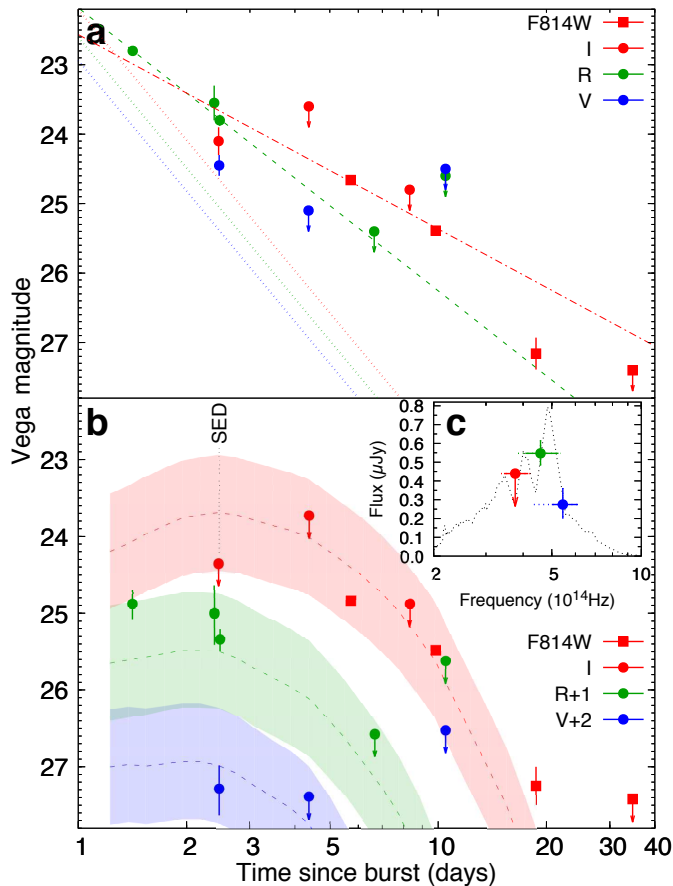


FIG. 1: **The optical observations of sGRB 050709 (a) and a comparison of the data with a theoretical macronova light curve (b).** (a): The fits to the R -band emission (green dashed line) and to the I -band observations from the VLT I -band data as well as the first two HST F814W-band data points (red dash-dotted line) yield the declines of $t^{-1.63 \pm 0.16}$ and $t^{-1.12 \pm 0.09}$, respectively. The dotted lines represent the “suggested”-afterglow emission lightcurves of the GRB outflow after the jet break (i.e., $t^{-2.5}$ for the energy distribution index of the shock-accelerated electrons $p \sim 2.5$). (b): Shown are the residuals of the optical emission after the subtraction of a suggested fast-declining forward shock afterglow after $t = 1.4$ days (dotted lines in the upper panel). The simulated $I/R/V$ -band macronova light curves [17] are for the ejecta from a black hole–neutron star merger, corresponding to an ejection mass of $M_{\text{ej}} \sim 0.05 M_{\odot}$ and a velocity of $V_{\text{ej}} \sim 0.2c$. An uncertainty of ~ 0.75 mag (the shaded region) has been adopted following Hotokezaka et al [32]. (c): The SED of the macronova signal of sGRB 050709 measured by VLT on July 12, 2005 compared with a possible Iron line-like spectral structure adopted from Kasen et al. [13]. Note that all errors are 1σ statistical errors and the upper limits are at the 3σ confidence level.

suggested-afterglow component has been subtracted) is very similar to that identified in hGRB 060614 [26].

In Fig.1(b) we compared the observed lightcurves with the predictions of a macronova model. Shown are the residual of the optical emission after the subtraction of a suggested forward shock afterglow with a fast declining emission after $t = 1.4$ days and the theoretical lightcurves of a macronova following a black hole–neutron star merger [17] with $M_{\text{ej}} \sim 0.05 M_{\odot}$ and $v_{\text{ej}} \sim 0.2c$, where c is the speed of light, M_{ej} and v_{ej} are the ejecta mass and velocity, respectively. This is comparable but slightly smaller than the parameters used for fitting the I -band excess observed in the afterglow of GRB 060614 [25]. Such a large amount of r -process material is consistent with a black-hole neutron star mergers [36–39] and it also supports the hypothesis that compact object mergers are prime sites of significant production of r -process elements [3, 40–46]. The black-hole neutron star merger scenario also has a significant implication on the prospect of establishing the GRB/GW connection in the advanced LIGO/Virgo era [47].

The weak I -band emission at $t \sim 2.5$ days together with the almost simultaneous R and V observations, implies a puzzling broad line-like structure (see Fig.1(c) for the afterglow-subtracted SED). A speculative interpretation is that this signal is due to a disk wind driven macronova. A strong line feature can be produced by a macronova dominated by Iron [13]. Such an Iron-group dominated macronova may arise from an accretion disk wind [48] in which the heavier r -process elements are depleted because strong neutrino irradiation from a remnant neutron star or the accretion torus can increase the electron fraction of the disk material. An interesting possibility is that the sub-relativistic neutron-rich ejecta from the compact object mergers may have a heavier or lighter composition in different directions and the resulting signal may be a combination of macronovae resulting from those (e.g. [49, 50]). A telescope of the E-ELT (European Extremely Large Telescope) class will be able to carry out spectroscopy of these faint signals allowing a better understanding of the phenomena.

Before concluding we note that if we do not rely on the re-analysis of the data, and adopt the afterglow interpretation of Watson et al. [28], even in this case there is an I band excess at 9.8 days. The most natural explanation for this excess is also a macronova and the physical parameters are similar to that adopted in the modeling of Fig.1.

B. Macronovae are ubiquitous in afterglows of short and hybrid GRBs

Following the tentative discovery of a third macronova signal we have re-examined all nearby sGRBs and hGRBs to search for possible macronova signals. Usually the macronova optical spectrum is expected to be soft, therefore ground-based deep I -band observations (ground-

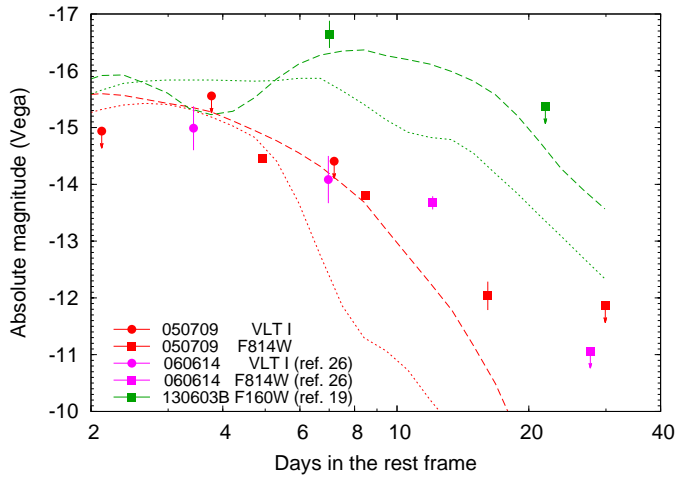


FIG. 2: **Comparison of the lightcurves of macronova candidates and theoretical models.** Absolute Vega magnitudes versus rest frame time of the macronova candidates in sGRB 050709, hGRB 060614 [26] and sGRB 130603B [19]. The red dashed line is the same as the dynamical ejecta macronova model *I*-band emission presented in Fig.1 (the green dashed line represents the *H*-band emission) while the red dotted line is the disk-wind ejecta macronova model *I*-band emission light curve [35] for $M_{\text{ej}} = 0.03 M_{\odot}$ and $V_{\text{ej}} = 0.07c$ (the green dotted line represents the *H*-band emission). Note that all errors are 1σ statistical errors and the upper limits are at the 3σ confidence level.

based *J/H/K*-band observations usually are not deep enough) as well as HST nIR observations are essential. The macronova candidates emerged in the sGRB 130603B, hGRB 060614 and sGRB 050709 lightcurves 1-2 weeks after the GRB triggers. At earlier times the forward shock afterglow emission outshines the macronova component while at late times the macronova emission also faded away. Hence we need deep *I*-band or near-infrared HST observations in the time interval of $\sim 5 - 15$ days. Theoretical predictions for macronovae vary significantly depending on the ejecta mass M_{ej} , the velocity V_{ej} , the composition, the merger types, and different observing angles (see e.g. Fig.10 of [14] and Fig.9 of [17] for illustration). For a reference we note that the observed signatures were ~ 24.5 Vega mag at about 9 days in F160W (*H*) band for sGRB 130603B at redshift 0.356, ~ 25 Vega mag at about 13.5 days in F814W (*I*) band for hGRB 060614 at redshift 0.125 and ~ 25 mag (Vega) at about 10 days in F814W(*I*) band for sGRB 050709 at redshift 0.16.

We focus on *Swift* and HETE-2 sGRBs and hGRBs at redshifts $z \leq 0.4$ since HST observations needed for such observations at higher redshifts are scarce [5, 51]. The initial “low redshift” sample consists of sGRBs 050509B, 050709, 050724, 060502B, 061201, 071227, 080905A, 130603B, 140903A, and 150101B and hGRBs 060505 and 060614 [5, 51]. Unfortunately most of these GRBs are not suitable and have to be excluded from

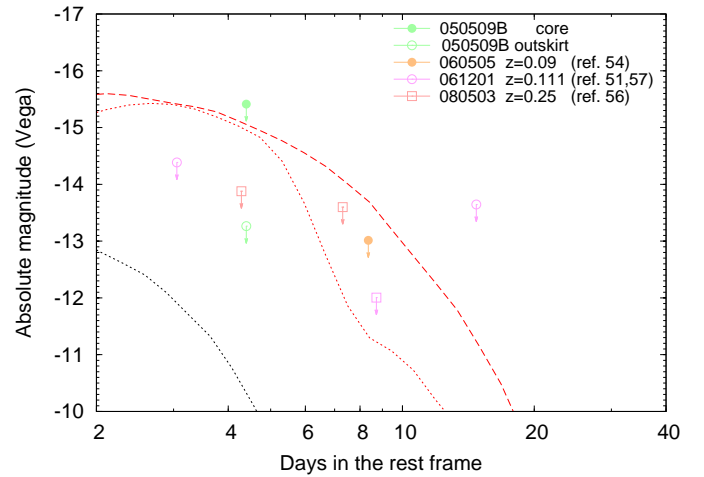


FIG. 3: **Comparison of the limits of macronova in some sGRBs and theoretical models.** Absolute Vega magnitudes versus rest frame time of the *I*-band/F814W-band observations of sGRB 050509B, hGRB 060505 [54] and sGRB 061201 [51, 57]. The HST F814W 3σ upper limits of GRB 080503 [56] are also shown for an assumed redshift of $z = 0.25$, following Kasen et al. [49]. Note that the Gemini *i*-band 3σ upper limit of sGRB 060505 was re-analyzed in this work. The red dashed line is the dynamical ejecta macronova model *I*-band emission while the red solid line is the disk-wind ejecta macronova model *I*-band emission light curve, where the same model parameters in Fig.2 are chosen. The black dotted line represents the macronova *I*-band emission expected for a double neutron star merger [14] with $M_{\text{ej}} = 0.01 M_{\odot}$ and $V_{\text{ej}} \sim 0.1c$, implying that the 3σ upper limits reported in sGRB 050509B, hGRB 060505 [54] and sGRB 061201 are not deep enough to exclude the compact object merger origin.

the “macronova candidates” sample. There were no observations within the macronova phase for sGRBs 050724, 060502B, 071227, 080905A and 140903A. No such observations were published yet for sGRB 150101B. The *I*/nIR observation information of the remaining events, sGRBs 050509B, 050709, 061201 and 130603B and hGRBs 060505 and 060614 are summarized in Supplementary Table 1 (see the Supplementary Information). Three events, sGRBs 050509B, 061201 and hGRB 060505 are potentially interesting but each one has its own caveat. The suggested host galaxy of sGRB 050509B is very bright and no optical counterpart had been detected. Hence the upper limits on the “underlying” afterglow and macronova emission sensitively depend on the unknown location within the host galaxy (see also [30]). The redshift of GRB 061201 is not secure [52] and it is possible that it was not sufficiently nearby. Using the hardness and prompt duration distribution Bromberg et al. [53] estimate that hGRB 060505 has a $97^{+2}_{-22}\%$ probability of being a Collapsar (see also the argument based on the location of the burst within a bright star forming region [54] and host galaxy observations [55]).

Therefore, in total there are just three or at most six

events that are sufficiently nearby and have sufficient data for a macronova identification. In the three of those (sGRB 050709, hGRB 060614 and sGRB 130603B) there are macronovae signatures (see Fig.2). In the three others potentially interesting events (sGRB 050509B, hGRB 060505 and sGRB 061201) there are only upper limits (see Fig.3) but it is possible that none of them is sufficiently binding. In the most “optimistic” case there are 3 macronovae in a sample consisting of just three events and the 95% confidence interval of the probability of a macronova taking place in a sGRB/hGRB is (0.47, 1). While in the most “pessimistic” case (i.e., there are 3 macronovae in a sample consisting of six GRBs) the 95% confidence interval for the probability is (0.18, 0.82). Therefore the detection prospect of macronovae in merger-powered GRBs are indeed encouraging though the fraction as low as ~ 0.18 cannot be ruled out.

Within this context it is interesting to mention also GRB 080503. It is not in our sample as its redshift is unknown [56]. Though no *I*-band/F814W-band or redder emission had been measured (see Fig.3, where the upper limits on the infrared luminosity are for a redshift $z \sim 0.25$, as assumed by Kasen et al. [49]), in optical bands the afterglow was detected in the time interval of $\sim 1.08 - 5.36$ days after the GRB trigger. The emission is quite blue, which is at odds with the dynamical ejecta macronova model but may be consistent with the disk-wind macronova model [49]. The potential challenge for this model is the non-identification of a nearby host galaxy as close as $z \sim 0.25$ in the deep HST/WFPC2 observation data of GRB 080503 [56].

It is interesting to compare now the observed features of the three macronova candidates. As far as the prompt emission is concerned, GRB 050709, a short burst with extended soft X-ray emission, bridges the gap between the canonical sGRB 130603B and the hGRB 060614 (see Table 1). The isotropic-equivalent prompt emission energy $E_{\gamma, \text{iso}}$ of sGRB 050709 is about 30 times smaller than that of hGRB 060614 and sGRB 130603B, while the macronova emission of sGRB 050709 is similar to that of hGRB 060614 (see Fig.2). The high energy transients were powered by a relativistic jet emerging from the central engine while the macronova emission arises from the *r*-process material ejected during the merger. The similarity between the macronova emission of sGRB 050709 and hGRB 060614 that had a very different energy release in the prompt phase suggests that the launch processes of the ultra-relativistic outflows and the sub-relativistic outflows are not related.

At $t \sim 16$ days after the trigger of sGRB 050709 there was an X-ray flare [27]. While at $t > 1.4$ days after the trigger of hGRB 060614, the X-ray afterglow is well behaved [34]. At $t \gtrsim 1$ days after the trigger of GRB 130603B, the X-ray emission became flattened [51]. The ratio between the macronova and X-ray radiation luminosities at the peak time of the macronova emission (i.e., $\mathcal{R}_{\text{MN/X}}$) varies from burst to burst by up to a factor of 10.

For sGRB 050709, hGRB 060614 and sGRB 130603B, the $\mathcal{R}_{\text{MN/X}}$ are $\sim (1, 0.1, 0.4)$, respectively, which could shed some lights on the physical origin (see below).

A remarkable feature shown in Fig.2 is the comparable peak luminosities of the different macronovae (i.e., $\sim 10^{41}$ erg s $^{-1}$). However, the macronovae associated with sGRB 050709 and hGRB 060614 were mainly identified in *I*/F814W-band, which are “bluer” than the F160W-band macronova component of sGRB 130603B. As in none of the cases we have a complete spectrum it is not clear if there was a real difference in the spectra.

III. DISCUSSION

The possible identification of three macronova candidates in a small sample containing just three or at most six events that are suitable for the search indicates that macronovae are common in sGRBs and hGRBs. Given the paucity of data for other events, macronovae could possibly arise in all sGRBs though a macronova fraction as low as ~ 0.18 can not be ruled out. A common feature of the macronova candidates is that the peak luminosity of macronovae is $\sim 10^{40} - 10^{41}$ erg s $^{-1}$ in the optical to infrared bands with a timescale of one week. In the compact binary merger scenario of sGRBs, this can arise from dynamical ejecta with heavy *r*-process elements, or lanthanide-free wind, or central engine activity. Here we discuss implications to each model.

The *I*-band light curve arising from dynamical ejecta with a mass of $0.05 M_{\odot}$ and an average velocity of $0.2c$ (see the black-hole neutron star merger model H4Q3a75 in [17] and also [58]) is shown in Fig.1 and Fig.2 as an example. Because of a fast expansion velocity and the large opacity of ≈ 10 cm 2 g $^{-1}$, the temperature is already low around the peak time and most of the photons are radiated in the near infrared *J*, *H*, and *K*-bands. The luminosity in the *I*-band is smaller than that in the *H*-band by a factor of 3–10 at 1 week after merger. This model can reproduce the observed *I*-band data of sGRB 050709 and the hGRB 060614 and the *H*-band data of sGRB 130603B with $\sim (0.05 M_{\odot}, 0.1 M_{\odot}, 0.03 M_{\odot})$, respectively. The massive ejecta with $\gtrsim 0.05 M_{\odot}$ suggests that the progenitor of sGRB 050709 is a black-hole neutron star merger [36–39]. However we should note that this estimate can change by a factor of a few due to uncertainties in the opacity, nuclear heating, and ejecta morphology. The upper limit in the *I*-band at 3 days of sGRB 061201 constrains the maximally allowed mass of dynamical ejecta as $\approx 0.02 M_{\odot}$ if the redshift of 0.111 is correct. The upper limits in the *I* band of hGRB 060505 are both consistent with almost $0.05 M_{\odot}$ and can be even higher if absorption at the host galaxy was significant [54]. Interestingly [54] was the first to search for a macronova signature in the afterglow light curve of this burst.

The absence of lanthanides in a wind reduces the opacity. The resulting macronova has a brighter and bluer

Table 1. Physical properties of GRBs/macronovae/afterglows with known redshifts.

	GRB 050709 ^a	GRB 060614 ^b	GRB 130603B ^c
$E_{\gamma, \text{iso}}$ (10^{51} erg)	0.069	2.5	2.1
z	0.16	0.125	0.356
Duration ^d (s)	0.5 (+130)	5 (+97)	0.18
Classification	sGRB + extended X-rays	hGRB	sGRB
Identifying macronova	in <i>I</i> /F814W	in <i>I</i> /F814W	in F160W
Macronova peak luminosity	$\sim 10^{41}$ erg s ⁻¹ (<i>I</i>)	$\sim 10^{41}$ erg s ⁻¹ (<i>I</i>)	$\sim 10^{41}$ erg s ⁻¹ (F160W)
M_{ej} ^e	$\sim 0.05 M_{\odot}$	$\sim 0.1 M_{\odot}$	$\sim 0.03 M_{\odot}$
$\mathcal{R}_{\text{MN/X}}$ ^f	~ 1	~ 0.1	~ 0.4

Note: a. Villasenor et al.[29] and this work; b. Gehrels et al. [21], Yang et al. [25] and Jin et al. [26]; c. Tanvir et al. [19], Berger [20] and Hotokezaka et al. [32]; d. The durations include that of the hard spike and the “extended emission” (in the bracket); e. The M_{ej} is estimated from the dynamical ejecta model and the value can change by a factor of a few due to uncertainties in the opacity, nuclear heating, and ejecta morphology; f. $\mathcal{R}_{\text{MN/X}}$ denotes the ratio between the macronova “peak” luminosity and the simultaneous X-ray luminosity.

peak luminosity on a shorter timescale [13, 14, 49, 50, 59]. Figure 2 shows the *I*-band light curve arising from a lanthanide-free wind with a mass of $0.03M_{\odot}$ and an average velocity of $0.07c$, where elements with atomic numbers of 31 – 54 are included (see the wind model in [14] and also [49]). This model can reproduce the *I*-band data of GRB 050709 and 060614 at early times ($t < 5$ days). However, the light curve at late times is faint compared to the data. While increasing the wind mass raises the late *I*-band luminosity, such a model is too bright to be compatible with the early *I*-band data ($t < 5$ days). The *I*-band upper limit at 3 days of GRB 061201 indicates the mass of a lanthanide-free wind of $\lesssim 0.01M_{\odot}$. The upper limits on the afterglow of hGRB 060505 were taken much later after the bursts and as such the implied limits on the wind ejecta are weak.

The central engine can also power a macronova. Here we focus on the X-ray powered macronova model [60] since this model is testable with the observed X-ray and optical data. In this model, X-ray photons emitted by the central engine are absorbed by the ejecta and re-emitted in the optical-infrared bands. Note that *r*-process material with a mass of $\gtrsim 10^{-3}M_{\odot}$ is required in order to keep the ejecta optically thick to optical photons until one week after the merger. While the spectrum and light curve of this emission are unclear, a relation of $L_{\text{IR}} \approx 0.1L_X$ (i.e., $\mathcal{R}_{\text{MN/X}} \approx 0.1$) is expected in this scenario. As summarized in Table 1, $\mathcal{R}_{\text{MN/X}}$ varies among the events. In particular, for GRB 050709, it is difficult to explain the macronova luminosity with $\mathcal{R}_{\text{MN/X}} \approx 1$. However, the flare activity in X-ray at late times may provide enough energy to produce the *I*-band emission. Better data in both X-ray and optical-IR at late times are needed to further test the X-ray powered macronova model.

The comprehensive examination of the near-infrared data of current nearby sGRBs and hGRBs yielded in total three or at most six events suitable for macronova searches. The successful identification of three candidates in such a limited sample demonstrates that macronovae arise in most if not all compact object merger events that produce GRBs. A comparison of the above

three scenarios favors the by now “standard” dynamical ejecta that is enriched by *r*-process elements [11, 37, 61]. The massive *r*-process material ejecta inferred in each one of these events strongly suggest that compact object mergers are the significant or even prime sites of producing heavy *r*-process elements [3, 40–46].

These results have important implications on the future of macronovae and GW electromagnetic counterparts observations (see e.g., [62, 63] for search strategies). Among the three macronova candidates, two were identified in *I*-band (there was also evidence for emission in R-band emission, too). Ground-based telescopes are much more sensitive in *I*-band than in *J/H/K*-bands. If the mergers powering sGRB 050709 and hGRB 060614 took place at luminosity distances of ~ 200 Mpc (the horizon of advanced LIGO/Virgo network for double neutron star mergers) or ~ 350 Mpc (the horizon of advanced LIGO/Virgo network for a neutron star merger with a $\sim 6 M_{\odot}$ black hole), the corresponding peak *I*-band emission is expected to be as bright as $\sim 21 - 22$ th magnitude or $\sim 22 - 23$ th magnitude, respectively. Such events are marginally detectable by new and upcoming transient surveys such as the ESO VLT Survey Telescope (VST, <https://www.eso.org/sci/facilities/paranal/telescopes/vst.html>, see Abbott et al.[64]) and the Zwicky Transient Facility (ZTF) that is expected to have first light in 2017 (<http://www.ptf.caltech.edu/ztf>). The Large Synoptic Survey Telescope (LSST; [65]) with a 9.6 deg^2 field of view that can image about 10^4 deg^2 of the sky in three clear nights down to limiting magnitude of $i \sim 23.5$ (Vega system), in principle, could easily identify such signals.

IV. METHODS

A. Optical and infrared data reduction

The VLT imaging data of GRB 050709 are publicly available in ESO Science Archive Facility (<http://archive.eso.org>). We reduce the raw data following the standard procedures in IRAF (<http://iraf.noao.edu>), including bias subtraction, flat fielding and image combination. Observations made with the same filter at different epochs are firstly aligned to the last epoch (reference frame), using the *imalign* tool in IRAF. The task *ficnv* in software package FITSH (<http://fitsh.szofi.net>) is used to convolve the reference to match the profile and brightness of objects in earlier frames. For each earlier frame, the reference frames is convolved to and subtracted. In this method, the object profile and zero point of the subtracted image are the same as the image that has been subtracted. Finally the aperture photometry is applied to the residual images and find the instrumental magnitudes of the afterglow. Photometric errors are estimated from the photon noise and the sky variance to 1σ confidence level. The 3σ of the background RMS of the residual images is taken as the limiting magnitude. Eight to ten point like objects in the field are used as reference stars for differential photometry. Finally, standard stars observed on July 12 and 30, 2005 were used for the absolute calibration. The results are presented in Table IV A, consistent with that reported in the literature [31]. The main novel result is the detection of the *I*-band emission at $t \sim 2.4$ day after the trigger of the GRB (see Fig.4). Our “new” detection is mainly benefited from the improvement on the change of the reference frame (i.e., from July 18 FORS1 observation to July 30 FORS2 observation). The advantage is less “contamination” from emission of the source (about 25.2 Mag versus > 27.2 Mag, according to

the HST observation), the original and reference images are both from the same instrument (FORS2) on VLT. Hence the signal to noise rate of the source is improved.

Note that in the direction of the burst, the Galactic extinction is expected to be just $E(B - V) = 0.01$ mag [66]. The optical afterglow of GRB 050709 is superposed on the outskirts of the host galaxy and the extinction is probably very small (i.e., ≤ 0.1 mag), too [27]. Therefore in this work, we ignore the extinction corrections of the optical data. We have also analyzed the Gemini-N r' -band data. In total there are two sets of exposures (i.e., 4×300 s on Jul 16 and 6×200 s on Jul 28). However the second sets of exposures have a high sky brightness (≈ 19.35 Vega Mag arcsec $^{-2}$) that is not suitable for reference frame in the image subtraction. Therefore, we performed image subtraction between the high-quality Gemini-N (on Jul 16) and VLT (on Jul 30) observations and got an upper limit (see Table 2).

We download the public HST archive data of GRB 050709 from the Mikulski Archive for Space Telescopes (MAST; <http://archive.stsci.edu>), including five observations with ACS in F814W band. The reduced data provided by MAST were used in our analysis. The last observation is taken as the reference and the other images of the same filter are subtracted in order to directly measure fluxes of the afterglow from the residual images. Aperture photometry was carried out for the afterglow in the residual image. The ACS zeropoints were used for absolute calibration. If the signal of the afterglow is too faint to be a secure detection, an upper limit of 3σ background RMS is adopted. Our results are summarized in Table 2, nicely in agreement with Fox et al. [27].

Danish 1.54m telescope data are not publicly available, and therefore we simply adopt the data reported in Hjorth et al. [30]. Table 2 is a complete list of the data points used in our analysis.

-
- [1] Abadie, J., Abadie, J., Abbott, B. P., et al. TOPICAL REVIEW: Predictions for the rates of compact binary coalescences observable by ground-based gravitational-wave detectors *CQGra*, **27**, 173001 (2010).
 - [2] Abbott, B. P., et al. (LIGO Scientific Collaboration, Virgo Collaboration). Prospects for Observing and Localizing Gravitational-Wave Transients with Advanced LIGO and Advanced Virgo. *Living Reviews in Relativity*, **19**, 1 (2016).
 - [3] Eichler, D., Livio, M., Piran, T., & Schramm, D. N., Nucleosynthesis, neutrino bursts and gamma-rays from coalescing neutron stars. *Nature*, **340**, 126-128 (1989).
 - [4] Nakar, E., Short-hard gamma-ray bursts. *Phys. Rep.*, **442**, 166-236 (2007).
 - [5] Berger, E. et al. Short-Duration Gamma-Ray Bursts. *Ann. Rev. Astron. Astrophys.*, **52**, 43-105 (2014).
 - [6] Li, L. X., and Paczyński, B. Transient Events from Neutron Star Mergers. *Astrophys. J. Lett.*, **507**, L59-L62 (1998).
 - [7] Kulkarni, S. R.. Modeling Supernova-like Explosions Associated with Gamma-ray Bursts with Short Durations. Preprint at <http://arxiv.org/abs/astro-ph/0510256> (2005).
 - [8] Rosswog, S. Mergers of Neutron Star-Black Hole Binaries with Small Mass Ratios: Nucleosynthesis, Gamma-Ray Bursts, and Electromagnetic Transients. *Astrophys. J.*, **634**, 1202-1213 (2005).
 - [9] Metzger, B. D. et al. Electromagnetic counterparts of compact object mergers powered by the radioactive decay of r-process nuclei. *Mon. Not. R. Astron. Soc.*, **406**, 2650-2662 (2010).
 - [10] Roberts, L. F., Kasen, D., Lee, W. H., & Ramirez-Ruiz, E. Electromagnetic Transients Powered by Nuclear Decay in the Tidal Tails of Coalescing Compact Binaries *Astrophys. J.*, **736**, L21 (2011)
 - [11] Korobkin, O., Rosswog, S., Arcones, A., & Winteler, C. On the astrophysical robustness of the neutron star merger r-process. *Mon. Not. R. Astron. Soc.*, **426**, 1940-

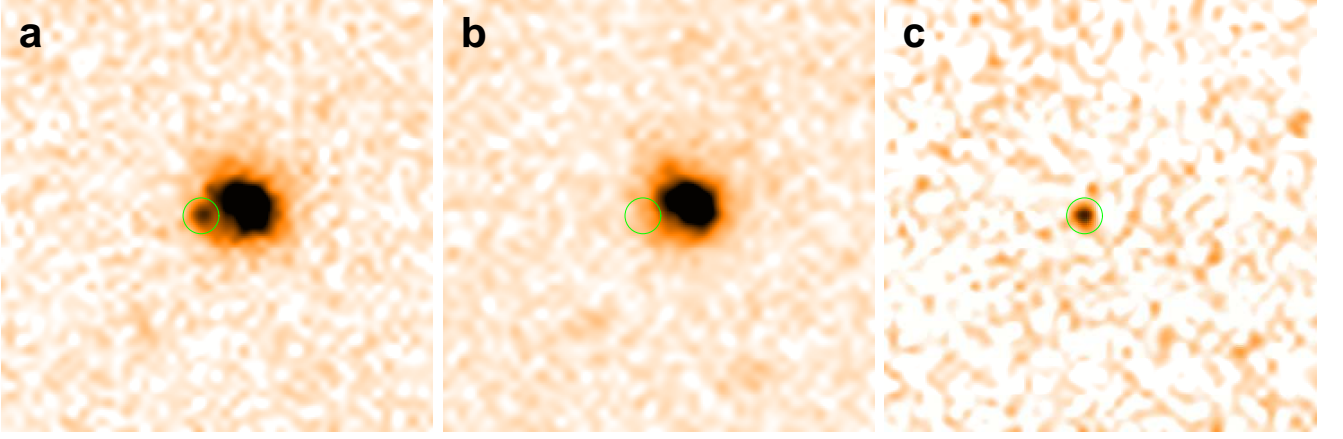


FIG. 4: **The VLT I band images of the afterglow of GRB 050709.** The data were taken on July 12 2005 (a) and July 30 2005 (b), and the signal resulted in the image subtraction (c). The afterglow position has been circled and the afterglow emission is clearly visible on July 12, 2005. The images are magnified only for demonstration.

Table 2. The optical observations of GRB 050709

Time (days)	Exposure (seconds)	Filter	Magnitude ^a (Vega)	Flux (μ Jy)	Seeing (arcsec)	Sky brightness ^b
2.46346	60×5^c	VLT/FORS2/V	24.45 ± 0.15	0.59 ± 0.08	0.76	21.79
4.36416	120×3	VLT/FORS1/V	> 25.1	< 0.31	0.89	21.55
10.48568	120×3	VLT/FORS1/V	> 24.5	< 0.55	0.73	19.49
20.16693	180×3	VLT/FORS2/V	—	—	0.66	21.46
2.47249	60×5	VLT/FORS2/R	23.80 ± 0.08	0.90 ± 0.07	0.68	21.19
6.64339	300×4^d	Gemini-N/r'(R)	> 25.4	< 0.20	0.67	20.93
10.47943	120×3	VLT/FORS1/R	> 24.6	< 0.43	0.59	19.26
20.17874	180×15^c	VLT/FORS2/R	—	—	0.61	20.97
2.45513	100×6	VLT/FORS2/I	24.1 ± 0.2	0.55 ± 0.09	0.65	19.85
4.37179	100×3	VLT/FORS1/I	> 23.6	< 0.86	0.79	19.51
8.33429	120×10	VLT/FORS1/I	> 24.8	< 0.30	0.42	19.40
20.23152	180×3	VLT/FORS2/I	—	—	0.61	19.73
5.71410	6360	HST F814W	24.66 ± 0.03^e	0.330 ± 0.009		
9.84385	6360	HST F814W	25.39 ± 0.05^e	0.169 ± 0.008		
18.70269	6360	HST F814W	27.16 ± 0.23^e	0.033 ± 0.008		
34.69556	6360	HST F814W	$> 27.4^e$	< 0.026		
371.78780	7039	HST F814W	—	—		
1.4166	600×12	Danish/R	22.80 ± 0.07^f	2.34 ± 0.12		
2.3862	600×17	Danish/R	23.55 ± 0.25^f	1.17 ± 0.26		

Note: a. The magnitudes of the extracted optical transient, here magnitude errors are reported in 1σ and upper limits are 3σ .

b. In units of Vega Mag arcsec⁻².

c. Some images are not combined.

d. The Gemini-N r'-band upper limit has been converted into *R*-band.

e. Fox et al. [27] reported the AB magnitudes, which are larger than the corresponding Vega magnitudes by 0.42 mag.

f. These data are taken from Hjorth et al. [30].

1949 (2012).

- [12] Barnes, J., & Kasen, D. Effect of a High Opacity on the Light Curves of Radioactively Powered Transients from Compact Object Mergers. *Astrophys. J.*, **775**, 18 (2013).
- [13] Kasen, D., Badnell, N. R. & Barnes, J., Opacities and spectra of the r-process ejecta from neutron star mergers. *Astrophys. J.*, **774**, 25 (2013).
- [14] Tanaka, M., and Hotokezaka, K. Radiative Transfer Simulations of Neutron Star Merger Ejecta. *Astrophys. J.*, **775**, 113 (2013).

- [15] Piran, T., Nakar, E., and Rosswog, S. The electromagnetic signals of compact binary mergers. *Mon. Not. R. Astron. Soc.*, **430**, 2121-2136 (2013).
- [16] Grossman, D., Korobkin, O., Rosswog, S., and Piran, T. The long-term evolution of neutron star merger remnants - II. Radioactively powered transients. *Mon. Not. R. Astron. Soc.*, **439**, 757-770 (2014).
- [17] Tanaka, M. et al. Radioactively Powered Emission from Black Hole-Neutron Star Mergers. *Astrophys. J.*, **780**, 31 (2014).

- [18] Lippuner, J., & Roberts, L. F. r-process Lanthanide Production and Heating Rates in Kilonovae. *Astrophys. J.*, **815**, 82 (2015).
- [19] Tanvir, N. R. et al. A ‘kilonova’ associated with the short-duration gamma-ray burst GRB 130603B. *Nature*, **500**, 547-549 (2013).
- [20] Berger, E., Fong, W., and Chornock, R. An r-process Kilonova Associated with the Short-hard GRB 130603B. *Astrophys. J. Lett.*, **744**, L23 (2013).
- [21] Gehrels, N., et al., A new γ -ray burst classification scheme from GRB060614. *Nature*, **444**, 1044-1046 (2006).
- [22] Fynbo, J. P. U., et al. No supernovae associated with two long-duration gamma-ray bursts. *Nature*, **444**, 1047-1049 (2006).
- [23] Della Valle, M. et al. An enigmatic long-lasting gamma-ray burst not accompanied by a bright supernova. *Nature*, **444**, 1050-1052 (2006).
- [24] Gal-Yam, A. et al. A novel explosive process is required for the γ -ray burst GRB 060614. *Nature* **444**, 1053-1055 (2006).
- [25] Yang, B., et al. A possible macronova in the late afterglow of the long-short burst GRB 060614. *Nat. Commun.*, **6**, 7323 (2015).
- [26] Jin, Z. P. et al. The light curve of the macronova associated with the long-short burst GRB 060614. *Astrophys. J. Lett.*, **811**, L22 (2015).
- [27] Fox, D. B., et al. The afterglow of GRB 050709 and the nature of the short-hard γ -ray bursts. *Nature*, **437**, 845-850 (2005).
- [28] Watson, D. et al. Are short γ -ray bursts collimated? GRB 050709, a flare but no break. *Astron. Astrophys.*, **454**, L123-L126 (2006).
- [29] Villaseñor, J. S., et al. Discovery of the short γ -ray burst GRB 050709. *Nature*, **437**, 855-858 (2005).
- [30] Hjorth, J., et al. The optical afterglow of the short γ -ray burst GRB 050709. *Nature*, **437**, 859-861 (2005).
- [31] Covino, S., et al. Optical emission from GRB 050709: a short/hard GRB in a star-forming galaxy. *Astron. Astrophys.*, **447**, L5-L8 (2006).
- [32] Hotokezaka, K., et al. Progenitor models of the electromagnetic transient associated with the short gamma ray burst 130603B. *Astrophys. J. Lett.*, **778**, L16 (2013).
- [33] Piran, T. The physics of gamma-ray bursts. *Rev. Mod. Phys.*, **76**, 1143-1210 (2004).
- [34] Xu, D., et al. Is search of progenitors for supernovaeless gamma-ray bursts 060505 and 060614: re-examination of the afterglows. *Astrophys. J.*, **696**, 971-979, (2009).
- [35] Tanaka, M., et al. Kilonova/Macronova Emission from Compact Binary Mergers. *Advances in Astronomy*, **2016**, 6341974 (2016).
- [36] Foucart, F., et al. Neutron star-black hole mergers with a nuclear equation of state and neutrino cooling: Dependence in the binary parameters. *Phys. Rev. D*, **90**, 024026 (2014).
- [37] Just, O., Bauswein, A., Pulpillo, R. A., Goriely, S., & Janka, H.-T. Comprehensive nucleosynthesis analysis for ejecta of compact binary mergers. *Mon. Not. R. Astron. Soc.*, **448**, 541-567 (2015).
- [38] Kyutoku, K., Ioka, K., Okawa, H., Shibata, M., & Taniguchi, K. Dynamical mass ejection from black hole-neutron star binaries. *Phys. Rev. D*, **92**, 044028 (2015).
- [39] Kiuchi, K., Sekiguchi, Y., Kyutoku, K., Shibata, M., Taniguchi, K., & Wada, T. High resolution magnetohydrodynamic simulation of black hole-neutron star merger: Mass ejection and short gamma ray bursts. *Phys. Rev. D*, **92**, 064034 (2015).
- [40] Lattimer, J. M. & Schramm, D. N. Black-hole-neutron-star collisions. *Astrophys. J. Lett.* **192**, L145-L147 (1974).
- [41] Piran, T., Korobkin, O., & Rosswog, S. Implications of GRB 130603B and its macronova for r-process nucleosynthesis arXiv:1401.2166 (2014).
- [42] Hotokezaka, K., Piran, T., & Paul, M. Short-lived ^{244}Pu points to compact binary mergers as sites for heavy r-process nucleosynthesis. *Nat. Phys.*, **11**, 1042 (2015).
- [43] Shen, S., Cooke, R. J., Ramirez-Ruiz, E., Madau, P., Mayer, L., Guedes, J. The History of R-Process Enrichment in the Milky Way. *Astrophys. J.*, **807**, 115 (2015).
- [44] van de Voort, F., Quataert, E., Hopkins, P. F., Kereš, D., & Faucher-Giguère, C.-A. Galactic r-process enrichment by neutron star mergers in cosmological simulations of a Milky Way-mass galaxy. *Mon. Not. R. Astron. Soc.* **447**, 140-148 (2015).
- [45] Ishimaru, Y., Wanajo, S., Prantzos, N. Neutron Star Mergers as the Origin of r-process Elements in the Galactic Halo Based on the Sub-halo Clustering Scenario. *Astrophys. J.* **804**, L35 (2015).
- [46] Wehmeyer, B., Pignatari, M., & Thielemann, F.-K. Galactic evolution of rapid neutron capture process abundances: the inhomogeneous approach. *Mon. Not. R. Astron. Soc.* **452**, 1970-1981 (2015).
- [47] Li, X., Hu, Y. M., Fan, Y. Z., & Wei, D. M. GRB/GW association: long-short GRB candidates, time-lag, measuring gravitational wave velocity and testing Einstein’s equivalence principle. *Astrophys. J.* in press, arXiv:1601.00180 (2016).
- [48] Metzger, B. D., Piro, A. L., & Quataert, E. Nickel-rich outflows from accretion discs formed by the accretion-induced collapse of white dwarfs. *Mon. Not. R. Astron. Soc.*, **396**, 1659-1664 (2009).
- [49] Kasen, D., Fernández, R., Metzger, B. D. Kilonova light curves from the disc wind outflows of compact object mergers. *Mon. Not. R. Astron. Soc.*, **450**, 1777-1786 (2015).
- [50] Metzger, B. D., & Fernández, R. Red or blue? A potential kilonova imprint of the delay until black hole formation following a neutron star merger. *Mon. Not. R. Astron. Soc.*, **441**, 3444-3453 (2014).
- [51] Fong, W. F. et al. A Decade of Short-duration Gamma-Ray Burst Broadband Afterglows: Energetics, Circumburst Densities, and Jet Opening Angles. *Astrophys. J.*, **815**, 102 (2015).
- [52] D’Avanzo, P. et al. A complete sample of bright Swift short gamma-ray bursts. *Mon. Not. R. Astron. Soc.*, **442**, 2342-2356 (2014).
- [53] Bromberg, O., Nakar, E., Piran, T., & Sari, R. Short versus long and clapsars versus non-collapsars: a quantitative classification of Gamma-ray Bursts. *Astrophys. J.*, **764**, 179 (2013).
- [54] Ofek, E. O. et al. GRB 060505: A possible short-duration gamma-ray burst in a star-forming region at a redshift of 0.09. *Astrophys. J.*, **662**, 1129-1135 (2007).
- [55] Thöne, C. C., Christensen, L., Prochaska, J. X., Bloom, J. S., Gorosabel, J., Fynbo, J. P. U., Jakobsson, P., and Fruchter, A. S. The host of the SN-less GRB 060505 in high resolution. *Mon. Not. R. Astron. Soc.*, **441**, 2034-2048 (2014).
- [56] Perley, D. A., et al. GRB 080503: Implications of a naked short Gamma-ray Burst dominated by extended emis-

- sion. *Astrophys. J.*, **696**, 1871-1885 (2009).
- [57] Stratta, G., et al. A study of the prompt and afterglow emission of the short GRB 061201. *Astron. Astrophys.*, **474**, 827-835 (2007).
 - [58] Kawaguchi, K., Kyutoku, K., Shibata, M., & Tanaka, M. Models of Kilonova/macronova emission from black hole-neutron star mergers. *Astrophys. J.*, **825**, 52 (2016).
 - [59] Perego, A., Rosswog, S., Cabezón, R., M., Korobkin, O., Kappeli, R., Arcones, A., & Liebendorfer, M. Neutrino-driven winds from neutron star merger remnants *Mon. Not. R. Astron. Soc.*, **443**, 3134-3156 (2014).
 - [60] Kisaka, S., Ioka, K., & Nakar, E. X-ray-powered macronovae. *Astrophys. J.*, **818**, 104 (2016).
 - [61] Wanajo, S., Sekiguchi, Y., Nishimura, N., Kiuchi, K., Kyutoku, K. & Shibata, M., Production of All the r-process Nuclides in the Dynamical Ejecta of Neutron Star Mergers *Astrophys. J.*, **789**, L39 (2014)
 - [62] Nissanke, S., Kasliwal, M., & Georgieva, A. Identifying Elusive Electromagnetic Counterparts to Gravitational Wave Mergers: An End-to-end Simulation. *Astrophys. J.* **767**, 124 (2013).
 - [63] Cowperthwaite, P. S., & Berger, E. A Comprehensive Study of Detectability and Contamination in Deep Rapid Optical Searches for Gravitational Wave Counterparts. *Astrophys. J.* **814**, 25 (2015).
 - [64] Abbott, B. P., et al. Localization and broadband follow-up of the gravitational-wave transient GW150914. *Astrophys. J. Lett.*, **826**, L13 (2016)
 - [65] Ivezić, Z., et al. LSST: from Science Drivers to Reference Design and Anticipated Data Products. arXiv:0805.2366 (2008)
 - [66] Schlegel, D. J., Finkbeiner, D. P. & Davis, M. Maps of dust infrared emission for use in estimation of reddening and cosmic microwave background radiation foregrounds. *Astrophys. J.* **500**, 525-553 (1998).
 - [67] Malesani, D., et al. Multicolor observations of the afterglow of the short/hard GRB050724. *Astron. Astrophys.*, **473**, 77-84 (2007).
 - [68] Berger, E. A Short Gamma-ray Burst "No-host" Problem? Investigating Large Progenitor Offsets for Short GRBs with Optical Afterglows. *Astrophys. J.*, **722**, 1946-1961 (2010).
 - [69] D'Avanzo, P. et al. The optical afterglows and host galaxies of three short/hard gamma-ray bursts. *Astron. Astrophys.*, **498**, 711-721 (2009).
 - [70] Troja, E. et al. An achromatic break in the afterglow of the short GRB 140903A: evidence for a narrow jet. *Astrophys. J. submitted*, arXiv:1605.03573 (2016).
 - [71] Levan, A. J., et al. GRB 150101B/Swift J123205.1-105602: VLT observations and redshift. *GCN CIRCULAR*, 17281 (2015).
 - [72] van der Horst, A. J., et al. GRB 150101B/Swift J123205.1-105602: continued WSRT radio and VLT optical observations. *GCN CIRCULAR*, 17309 (2015).

V. END NOTES.

Acknowledgement. This work was supported in part by the National Basic Research Programme of China (No. 2013CB837000 and No. 2014CB845800), NSFC under grants 11525313 (i.e., Funds for Distinguished Young Scholars), 11361140349 (Joint NSFC-ISF Re-

search Program funded by the National Natural Science Foundation of China and the Israel Science Foundation), 11273063, 11433009, 11103084, and U1231101, the Chinese Academy of Sciences via the Strategic Priority Research Program (Grant No. XDB09000000) and the External Cooperation Program of BIC (No. 114332KYSB20160007), the Israel ISF–CNSF grant, the Templeton foundation and the I-Core center for excellence “Origins” of the ISF. SC has been supported by ASI grant I/004/11/0.

Author contribution. Y.Z.F, Z.P.J, S.C and T.P launched this project. Z.P.J, X.L (from PMO), S.C and P.D (from INAF/OAB) carried out the data analysis/statistics. K.H and T.P (from HU), M.T. (from NAOJ), Y.Z.F, Z.P.J and D.M.W (from PMO) interpreted the data. Y.Z.F, T.P, S.C and K.H prepared the paper and all authors joined the discussion.

Author information. Correspondence should be addressed to Y. Z. Fan (e-mail: yzfan@pmo.ac.cn), or S. Covino (e-mail: stefano.covino@brera.inaf.it), or T. Piran (e-mail: tsvi.piran@mail.huji.ac.il).

Competing financial interests. The authors declare no competing financial interests.

Supplementary discussion: the near-infrared observations of nearby sGRBs and hGRBs

In the second part of Sec. II we have a sample of 12 nearby sGRBs and hGRBs. The near-infrared observations of these events are summarized in Supplementary Table 1. Note that for the afterglow emission of GRB 150101B, there is still no formally published paper, yet, and we collect the information from GCN Circulars as well as the websites for 8-10m class telescopes and HST. For other events we collect the data reported in the literature. Below we explain in some detail why we conclude that sGRB 060502B, sGRB 050724, sGRB 071227, sGRB 080905A, sGRB 140903A and sGRB 150101B are not suitable for macronova identification. We also describe the HST observations of the afterglow emission of sGRB 050509B since they have not been formally reported in the literature yet.

- GRB 050509B: this burst had dense HST followup observations in F814W band on May 14, 18, 28 and June 1 2005 (<http://archive.stsci.edu>), each exposure lasted 6908 s. There is a very bright elliptical galaxy (~ 16 mag, $z = 0.225$) near the *Swift* XRT error box, likely to be the host galaxy. Without an identification of an optical counterpart, it is challenging to set a robust limit on the underlying macronova (see also [30] for similar conclusion on afterglow but based on the ground-based R/V observations). If the GRB is at the outskirts of the galaxy, the limit would be > 27.4 mag and can be used to constrain the merger scenario. However if it is in the inner core of the galaxy, the limit would be > 25.3 mag and the constraint on the macronova emission is weak.
- sGRB 050724: this burst had rare ground-based I -band observations and no HST followup observation, the large amount of dust extinction (i.e., $A_V \approx 2$ mag) [27, 67] in the direction of the burst is an important obstacle for macronova search, too.
- sGRB 060502B: the redshift of this burst is suggested to be either unknown [68] or 0.287 [5]. Assuming a redshift of 0.287, the main obstacle for macronova hunting is the lack of dense and deep optical/nIR observations and there was just a R -band flux upper limit $\leq 0.7\mu\text{Jy}$ at ~ 16.8 hours reported [68]. Considering its relatively high redshift, a macronova signal, if intrinsically as luminous as that identified in sGRB 050709, can just give rise to R -band peak emission of ~ 26 th mag, which is well below the single upper limit previously reported.
- sGRB 071227: this event had a relatively high redshift ($z = 0.381$) but had neither ground-based I -band observations nor HST followup observations [51].
- sGRB 080905A: the redshift of $z = 0.122$ is low that is suitable for macronova hunting. However, the latest two VLT/ R -band followup observations were on Sept 7 and 23, respectively [51]. Such rare observations, either too early or too late, are not helpful for macronova search (This is in particular the case for the NS-NS merger scenarios for which the peak R -band macronova emission is expected to be ~ 26 th mag for $M_{\text{ej}} \leq 0.01 M_{\odot}$ and $z \approx 0.1$ [13, 14].)
- sGRB 140903A: this burst was at $z = 0.351$, for which HST nIR observations are necessary to get the macronova signal. However, no HST exposure of the afterglow of GRB 140903A was performed, the available dataset is not deep enough to search for a macronova (also discussed in Troja et al [70]).
- sGRB 150101B: the redshift is $z = 0.134$. If the associated kilonova emission is similar to that of GRB 130603B, a H-band peak magnitude is expected to be around $H(\text{AB}) = 22 - 23$ [71]. The IR observations with VLT/HAWK-I on January 16 however found no evidence for any source to a preliminary limiting magnitude of $H(\text{AB}) > 23.5$ [72]. The macronova signal of GRB 130603B was detected at $t \sim 7$ day (in the burster's rest frame), the non-detection in GRB 150101B in H-band may be due to the long delay of the exposure. The TNG had two J-band measurements on Jan 11, Jan 15 2015, respectively. The obtained upper limits, however, are not tight enough to exclude the presence of a macronova as bright as that of GRB 130603B [51]. The VLT I -band observations were performed either too early or too late for the macronova detection. The first visit of HST in F606W-band was on 11 Feb. 2015, which is about 40 days after the GRB trigger, too late to catch the macronova signal.

Supplementary Table 1. The ‘nearby’ sGRBs and hGRBs with optical afterglow emission.

GRB	z	Ground-based I-band	HST nIR observations	Macronova search
050509B ^a	0.225		May 14, 18, 28 and Jun 1	Suitable (No)
050709 ^{a,b}	0.161	VLT/Jul 12, 14, 18, 30	Jul 15, 19, 28 and later	Suitable (Yes)
050724 ^{a,c}	0.257	VLT/Jul 25, 27, 30		Not Suitable
060502B ^d	0.287			Not Suitable
060505 ^e	0.089	Gemini-S/May 14	May 19 and Jun 06	Suitable (No)
060614 ^f	0.125	VLT/Jun 16, 17, 18 and later	Jun 28 and Jul 16	Suitable (Yes)
061201 ^{a,g}	0.111	VLT/Dec 2, 3, 5, 18	Dec. 11	Suitable (No)
071227 ^{a,h}	0.381			Not Suitable
080905A ^a	0.122			Not Suitable
130603B ^{a,i}	0.356	Gemini/Jun 4, 5	Jun 13 and Jul 03	Suitable (Yes)
140903A ^{a,j}	0.351	Gemini-N/Sep 5		Not Suitable
150101B ^{a,k}	0.134	VLT/Jan 4, 19, 20		Not Suitable

Note: a. Fong et al. [51]; b. Fox et al. [27] and Covino et al. [31]; c. Malesani et al. [67]; d. Berger et al. [68] e. Ofek et al. [54]; f. Della Valle et al. [23] and Gal-Yam et al. [24]; g. Stratta et al. [57]; h. D’Avanzo et al. [69]; i. Tanvir et al. [19]; j. Troja et al. [70]; k. Levan et al. [71].